

Molecular hydrogen in *a*-Si:H

Y. J. Chabal and C. K. N. Patel

AT&T Bell Laboratories, Murray Hill, New Jersey 07974

The past few years have seen a number of studies involving the presence of molecular hydrogen trapped in *a*-Si:H. The main techniques used have been nuclear magnetic resonance, calorimetry, and infrared absorption. The results suggest that H₂ is trapped in a number of samples in microbubbles (≈ 10 Å) under high pressure (≈ 2 kbar) at room temperature, solidifies around 25 K, and undergoes an orientational phase transition around 15 K. The data are reviewed here, and the effects that such H₂ microbubbles may have on the properties of *a*-Si:H are discussed.

CONTENTS

I. Introduction	835
II. Molecular H ₂ Clusters in <i>a</i> -Si:H	835
III. High-Pressure Molecular H ₂ and IR Measurements	837
A. Room-temperature data	837
B. Low-temperature data	838
IV. Recent NMR Studies: Nature of H ₂ in the Transition Region	840
V. Discussion	842
A. Nature of microvoids in <i>a</i> -Si:H	842
B. Hydrogen phase transitions and low-temperature phases	843
Acknowledgments	844
References	844

I. INTRODUCTION

The presence of molecular hydrogen in hydrogenated amorphous silicon (*a*-Si:H) has recently attracted attention because the state of the occluded H₂ molecule is unexpected and thought to be responsible for some of the properties attributed to amorphous silicon. Instead of being incorporated in a random and dilute way, as was first expected (Conradi and Norberg, 1981; Leopold *et al.*, 1982), the H₂ molecules are found to be mostly clustered in microbubbles (Chabal and Patel, 1984a; Graebner *et al.*, 1985) at relatively high pressures (Chabal and Patel, 1984a, 1984b).

The problems regarding H₂ in *a*-Si:H range from understanding the properties of these quantum rotors under such unusual conditions (high density at room temperature, solid under restricted geometry at low temperatures) to modeling the mechanisms by which such microbubbles can be formed during the growth of *a*-Si:H films. Several techniques such as nuclear magnetic resonance (NMR) (Conradi and Norberg, 1981; Reimer *et al.*, 1981; Carlos and Taylor, 1982; Leopold *et al.*, 1982, 1984; Boyce and Thompson, 1984; Lamotte, 1984; Vander Heiden *et al.*, 1984; Boyce and Stutzmann, 1985; Norberg, 1985; Fry *et al.*, 1987), calorimetry (Graebner *et al.*, 1984, 1985; Löhneysen *et al.*, 1984), and infrared (IR) spectroscopy (Chabal and Patel, 1984a, 1984b) have been used to tackle these problems. The results obtained so far have unraveled a number of details about the state of H₂ in *a*-Si:H and have provided a basis for a fairly consistent

description of the microbubbles. However, they are not yet sufficient to establish the governing processes for microbubble formation.

In this paper, we review the evidence obtained so far that has led to the identification and description of these microbubbles (Chabal and Patel, 1985). In Sec. II, we review the work that led to the establishment that H₂ clusters are present in *a*-Si:H. This work includes the early NMR studies (Taylor, 1984; Lamotte, 1985) and calorimetric studies. In Sec. III, we describe the IR studies that identified the high-pressure nature of these bubbles at room temperature and provided evidence for a gas/solid phase transition. In Sec. IV, the more recent NMR work is reviewed. This work reconciles the observation of the early NMR studies with those of the calorimetry and IR measurements regarding the amount of H₂ incorporated in *a*-Si:H. Furthermore, it uncovers the presence of an orientational phase transition at low temperatures. Finally, Sec. V addresses the problem of the nature of the microbubbles and the occluded H₂ in *a*-Si:H.

II. MOLECULAR H₂ CLUSTERS IN *a*-Si:H

The anomalous temperature dependence of the proton NMR spin-lattice relaxation time T_1 measured by Carlos and Taylor (1980) provided the first observation that led Conradi and Norberg (1981) to infer the presence of H₂ in *a*-Si:H. The strong temperature dependence of T_1 with a minimum observed around 40 K (Fig. 1) is not expected unless there is a relaxation process for the nuclear spins of the atomic H incorporated in *a*-Si:H. Because of the close resemblance of the T_1 temperature dependence to that of the phonon-dominated and much faster proton $T_1(\text{H}_2)$ of isolated H₂ in nonmagnetic hosts (Conradi *et al.*, 1979; Fedders, 1979), Conradi and Norberg argued that, among many possibilities involving diffusion, disorder modes, and paramagnetic centers, the T_1 minimum could be explained by the presence of a dilute system of fast-relaxing ortho-H₂ molecules. The T_1 temperature dependence (T^2 above $T_{1\text{min}}$ and faster than T^{-2} below) and the T_1 frequency dependence (independent of ω_0 above $T_{1\text{min}}$ and ω_0^2 below $T_{1\text{min}}$) led them to postulate that two phonon Raman processes relax the H₂ molecular rotational states, modulating the intramolecular dipolar

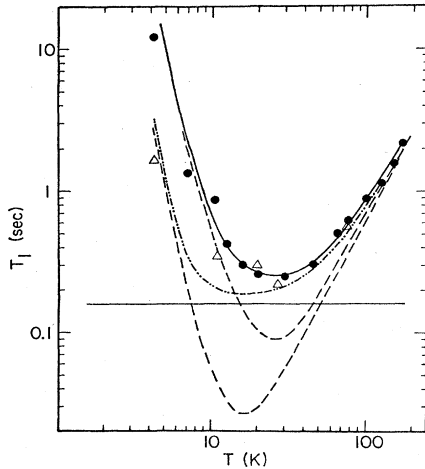


FIG. 1. Proton relaxation times below 200 K reported by Carlos and Taylor (1980) for *a*-Si:H at 42.3 MHz (solid dots) and at 12.3 MHz (triangles). The solid and dot-dashed lines are fits to the data (for 42.3 and 12.3 MHz, respectively) of a relaxation model proposed by Conradi and Norberg (1981) and described in the text. The horizontal line indicates a spin-diffusion bottleneck $T_1 = 0.16$ sec. The dashed lines indicate the calculated proton relaxation time (for 42.3 and 12.3 MHz, respectively) in the case of rapid spin diffusion ($T_1 \ll 0.01$ sec).

interactions and relaxing the protons of the H_2 . The majority of the protons in the sample would then relax to the ortho- H_2 by spin diffusion. They predicted that the T_1 minimum should be increased as ortho-para conversion took place at low temperature.

Their idea was tested by Carlos and Taylor (1982) who observed an increase in $T_{1\min}$ for samples held at 4.2 K as a function of time. Since H-spin relaxation can only occur via an orthohydrogen molecule, the $T_{1\min}$ is expected to increase as the statistical distribution of H_2 at room temperature (ortho/para=3) is modified at low temperature due to ortho-para conversion. The $T_{1\min}$ time dependence could be well described by a bimolecular process, in which the nuclear interaction between neighboring ortho-molecules governs the ortho-para conversion rate. The measured rate, $1 \times 10^{-2} \text{ h}^{-1}$, compared reasonably well to that of solid H_2 , $1.9 \times 10^{-2} \text{ h}^{-1}$. However, since the rate depends on the phonon spectrum of the host lattice as well as on the H_2 - H_2 distance, a description of the arrangement of these H_2 molecules in *a*-Si:H could not be inferred.

The concentration of molecular hydrogen in *a*-Si:H was extracted from the NMR data, assuming a uniform distribution of all hydrogen (atomic and molecular) in *a*-Si:H, and was found to be $\approx 2.5 \times 10^{19} \text{ H}_2/\text{cm}^3$, i.e., 0.05 at. % (Conradi and Norberg, 1981; Leopold *et al.*, 1982). The amount of molecular hydrogen determined by these early NMR measurements was anomalously low, being slightly less than 1% of the total hydrogen content in *a*-Si:H.

Shortly thereafter a series of calorimetry experiments,

performed at or below 5 K, showed that the amount of heat released during ortho-para conversion required the presence of up to an order of magnitude more H_2 , i.e., ≈ 0.5 at. %, to be accounted for (Graebner *et al.*, 1984; Löhneysen *et al.*, 1984). The assumptions were that the room-temperature concentration (ortho/para=3) was maintained during the rapid cooling, and that the heat released upon conversion was $k_B \times 170 \text{ K}$, i.e., its solid value (k_B is Boltzmann's constant). The concentration was found to depend both on the growth conditions and on the postannealing treatment. It was largest for samples grown by plasma decomposition of silane on substrates held at 230°C subjected to a 500°C postannealing.

The heat release was well fit by a bimolecular conversion mechanism over a period of 12 d for the samples annealed to 500°C as shown in Fig. 2 (Graebner *et al.*, 1985). The rate constant was $2.5 \times 10^{-2} \text{ h}^{-1}$. This rate is similar to that for solid H_2 , which varies from $1.9 \times 10^{-2} \text{ h}^{-1}$ at zero pressure to $3 \times 10^{-2} \text{ h}^{-1}$ at several kbar pressure. The ortho-para conversion mechanisms were therefore assumed to be similar. Since the bimolecular rate depends greatly on the intermolecular distance, a uniform distribution of H_2 in *a*-Si:H (average separation $\approx 20 \text{ \AA}$) would give a conversion rate orders of magnitude lower than the observed rate. It was therefore concluded that H_2 was clustered in *a*-Si:H. Further, a lower limit on the size of the clusters could be obtained from the ortho-para concentration for which a bimolecular decay could still be observed (after 12 d). A minimum of 10 H_2 per cluster was deduced.

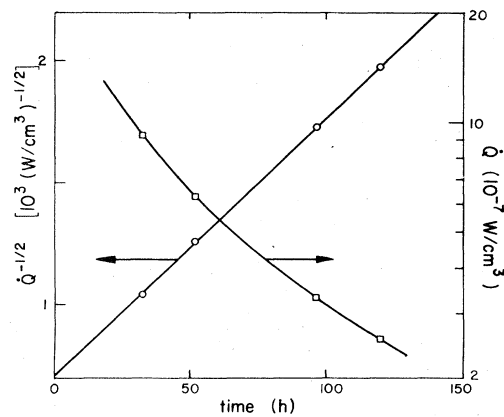


FIG. 2. Heat evolution \dot{Q} from *a*-Si:H annealed at 500°C obtained from calorimetry by Graebner *et al.* (1984). The zero of time corresponds to the beginning of cooling from 150 to 4.2 K. \dot{Q} is plotted in two ways: directly as \dot{Q} (squares), and as $\dot{Q}^{-1/2}$ (circles). The curved line drawn through the squares illustrates the nonexponential decay of \dot{Q} . The straight line drawn through the circles is indicative of a bimolecular rate equation, $\dot{x} = -cx^2$, where x is the fraction of H_2 in an ortho- H_2 form. The uncertainty in \dot{Q} is comparable to the size of the symbols. Measurements of \dot{Q} were extended to $\approx 300 \text{ h}$ (12 d; see Graebner *et al.*, 1985) and $\dot{Q}^{-1/2}$ was found to increase linearly in time during this time.

The specific heat was found to be dominated by a broad peak near 3.5 K. This peak is indicative of a short-range orientational order of ortho- H_2 within each cluster presumably due to electric-quadrupole-quadrupole (EQQ) interactions, as in bulk H_2 (Graebner *et al.*, 1985). However, the lack of a sharp peak in the heat capacity below 2 K precludes the establishment of long-range order, suggesting that the clusters must be strained.

The early NMR and calorimetry experiments therefore established that H_2 is contained in *a*-Si:H in the form of clusters. A lower limit on the cluster size ($> 10 H_2$) was set and short-range orientational ordering at low temperatures was inferred. However, the concentration of H_2 remained a puzzle. While calorimetry experiments (which are quite accurate and require reasonable assumptions) showed that the concentrations ranged from 0.1 to 0.5 at. %, the concentrations inferred from NMR were consistently lower (≈ 0.05 at. %) for similarly prepared samples. The resolution of this apparent conflict has come with the more recent NMR measurements and will be discussed in Sec. IV.

III. HIGH-PRESSURE MOLECULAR H_2 AND IR MEASUREMENTS

A. Room-temperature data

An isolated H_2 molecule is infrared inactive because it has a center of symmetry in the ground state. Infrared absorption arises from the dipole moment induced by the distortion of the electron distribution upon collisions with other molecules or atoms. The induced dipole moment is modulated by the vibrations and rotations of the collision partners. In general, this induced absorption is extremely weak.

Using total internal reflection on thin films of *a*-Si:H ($\approx 2 \mu\text{m}$) plasma deposited on crystalline silicon plates, an effective thickness of ≈ 0.5 mm could be probed. That length gave enough sensitivity to detect the weak IR absorption arising from molecular H_2 incorporated in *a*-Si:H (Chabal and Patel, 1984a).

Two salient features in the measured induced spectra taken on room-temperature samples (Fig. 3) gave precise information on the state of the occluded H_2 . The first was a notable absorption in a frequency range that originates from double transitions. Double transitions arise from simultaneous transitions in *two separate* H_2 molecules upon collision. For example, a double transition could involve a pure rotational quantum in one molecule with a vibrational and a rotational quantum in the other. This observation shows that H_2 is not isolated, but rather clustered as suggested by the calorimetry experiments.

The second feature deals with two aspects of the profile of the vibrational absorption spectrum. The first concerns the pure vibrational transition Q , which is clearly split at room temperature with a separation between the peaks $\Delta \equiv \nu_{Q_R} - \nu_{Q_P} = 240 \text{ cm}^{-1}$ about the expected value of $\nu_Q = 4155 \text{ cm}^{-1}$. This type of profile, which arises

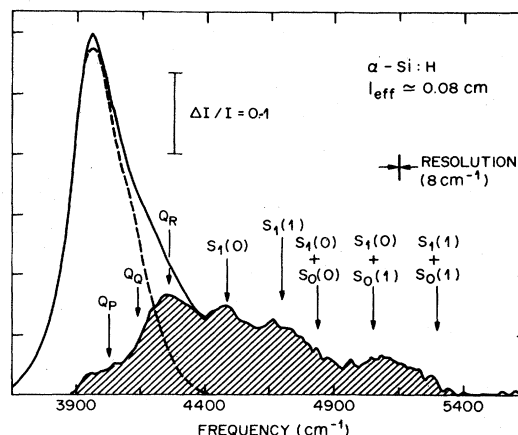


FIG. 3. Infrared absorption spectrum of *a*-Si:H in the region 3700–5600 cm^{-1} . The solid line shows the raw spectrum associated with *a*-Si:H (from Chabal and Patel, 1984a). The dashed curve is the contribution of the first overtone of the Si-H stretch mode obtained from measurements of the fundamental Si-H stretch at 2005 cm^{-1} (Chabal and Patel, 1984a). The hatched area, obtained by subtracting the overtone absorption from the raw absorption spectrum, corresponds to the infrared absorption associated with occluded H_2 in *a*-Si:H. The transitions labeled Q (Q_P, Q_Q, Q_R), $S_1(0)$, and $S_1(1)$ correspond to vibrational (Q) and vibrational-rotational (S_1) transitions taking place on *single* H_2 molecules. The *double* transitions, labeled S_1+S_0 , correspond to transitions requiring two H_2 molecules.

from the superposition of various single and double transitions, was shown by Van Kranendonk (1968) to exhibit a splitting due to an intercollisional interference effect. A destructive interference is established between the intercollisional and intracollisional part of the overlap-induced part of the dipole moment that dominates the Q branch absorption. The half-width of this collision-interference-induced dip is (Van Kranendonk, 1968)

$$\delta_c (\text{cm}^{-1}) = 1/2\pi c \tau_c, \quad (1)$$

where τ_c is the mean time between collisions. For a large range of densities, τ_c is proportional to N_{H_2} , the density of molecular hydrogen. In particular, at room temperature, the observed separation corresponds to $N_{H_2} = 2.2 \times 10^{22} \text{ H}_2/\text{cm}^3$ (≈ 800 amagat; see Hare and Welsh, 1958). This density corresponds to a pressure of 2 kbar and is similar to the density of solid H_2 , $N_{H_2}^s = 2.6 \times 10^{22} \text{ H}_2/\text{cm}^3$, at zero pressure.

The second relevant aspect of the profile is that of the observed width of the purely vibrational and vibrational-rotational lines. This width is a consequence of the short duration of the collisions and the uncertainty principle. The broad induced transition is in effect a continuum of summation and difference tones $\nu_m \pm \nu_k$, where ν_m is the molecular frequency and $h\nu_k$ the continuum of relative kinetic energies of the colliding pair. The intensities in the low- and high-frequency wings at frequencies displaced by $\pm \Delta\nu$ (in cm^{-1}) from ν_m are therefore related by the Boltzmann relation,

$$\frac{I(\nu_m - \Delta\nu)}{I(\nu_m + \Delta\nu)} = \exp(-\Delta\nu hc/kT), \quad (2)$$

which imparts a characteristic asymmetry to the profile of each transition. Both the width and the asymmetry of the observed bands indicate that high-pressure gas is occluded within pockets in *a*-Si:H.

The overall profile of the complete observed spectrum does not resemble that of H₂ trapped in a foreign gas (Hare and Welsh, 1958), a liquid, or a solid (see, e.g., Kriegler and Welsh, 1968), which display a much stronger *Q* branch relative to the vibrational-rotational branches. Therefore we conclude from the observed profiles that, if there is isolated H₂ in *a*-Si:H, it is a negligible fraction of the total H₂ amount.

The conclusion from the IR work at room temperature is that H₂ is incorporated in *a*-Si:H in the form of *high-pressure* bubbles. It is important to keep in mind that the IR absorption strength of H₂ depends on the square of the density. If there is a distribution of pressures among all these microbubbles, as is reasonable to assume, then the IR data will preferentially pick out the high part of the distribution. From the IR measurements alone therefore we cannot rule out that there is a wide distribution ranging from 0 to 2 kbar. However, the following analysis of the H₂ concentration would suggest that a large fraction of H₂ is at elevated pressures.

In order to relate the measured absorption to the total concentration of H₂ in *a*-Si:H, an optical sum rule may be used that takes into account local field enhancement. The general form that relates the observed extinction ratio, I/I_0 , to the total density of absorbing centers $N_{\text{H}_2}^{a\text{-Si}}$ is (Lax, 1952)

$$(E_{\text{eff}}/E)^2 \epsilon^{-1/2} \int_{\text{band}} (N_{\text{H}_2}^{a\text{-Si}}/N_{\text{H}_2}) \alpha_{\text{H}_2} d\nu = -l_{\text{eff}}^{-1} \int \ln(I/I_0) d\nu, \quad (3)$$

where ϵ is the dielectric constant of the *a*-Si:H at the frequencies considered ($\epsilon \approx 12$), α_{H_2} is the intrinsic absorption coefficient of H₂ gas under similar conditions (pressure corresponding to the density N_{H_2} and temperature), and l_{eff} is the experimentally determined effective length of *a*-Si:H probed by the IR beam. Estimates for the value of the local-field enhancement, E_{eff}/E , have been proposed for the case of H in *a*-Si:H without a great deal of success, as discussed by Cardona (1983). There are two main approaches. The first is the Onsager local-field approximation (Onsager, 1936), which treats the absorber as a point dipole in a spherical cavity within the dielectric medium. For weakly polarizable molecules, the result is

$$E_{\text{eff}}/E = \frac{3\epsilon}{2\epsilon + 1}. \quad (4)$$

The second approximation uses the Lorentz local fields, discussed by Dexter (1955), which treats the absorption of the molecules embedded in a dielectric medium resulting in

$$E_{\text{eff}}/E = \frac{\epsilon + 2}{3}. \quad (5)$$

This second approach was found to give a better description of the SiH absorption in *a*-Si:H, although the justification for using it may not be clear (Cardona, 1983). With the correction given in Eq. (5), and $N_{\text{H}_2} \approx 2.2 \times 10^{22}$ H₂/cm³ (800 amagat), we find that $N_{\text{H}_2}^{a\text{-Si}} \approx 10^{21}$ H₂/cm³ based on the value of the absorption coefficient $\alpha_{\text{H}_2} = 3.4$ cm⁻¹ for $N_{\text{H}_2} = 2.3 \times 10^{22}$ H₂/cm³ (850 amagat) as measured by Hare (Hare and Welsh, 1958). This corresponds to 2 at. %. For comparison, the Onsager local-field approximation [Eq. (4)] would give the unphysically large concentration of 20 at. %.

The reliability of the IR determination of H₂ concentration is therefore poor due to difficulties in taking into account local-field corrections. It is clear, however, that H₂ cannot be present predominantly at low pressures. At atmospheric pressure, the absorption would be 10⁶ times weaker and the density would have to be 10³ times larger to account for the observed absorption.

B. Low-temperature data

There are two regimes of interest at low temperatures. The first occurs in a moderately low temperature range (300–100 K) in which the silicon matrix can undergo changes due to thermal expansion, while H₂ gas or liquid will vary in an isotropic and well-established fashion. The second occurs at much lower temperatures (35–10 K), in which range the thermal expansion is completely negligible, but H₂ gas or liquid undergoes a phase transformation to a solid or “frozen-lattice” state.

Comparison of the infrared absorption spectra at 300 and 80 K (Fig. 4) reveals a much reduced absorption of

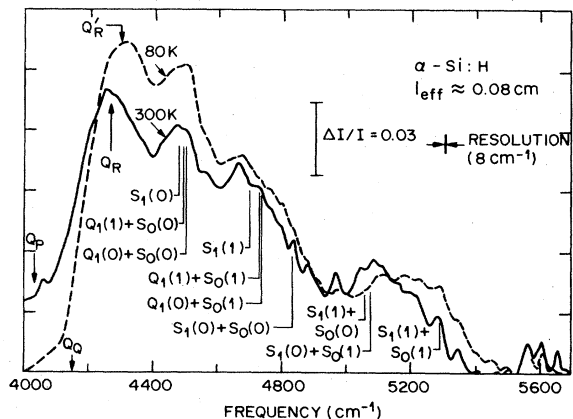


FIG. 4. Infrared absorption spectra of occluded H₂ gas in *a*-Si:H at 300 K (solid line) and 80 K (dashed lines), from Chabal and Patel (1984a). All the possible transitions are indicated. The notation $S_x(J)$ indicates that a purely rotational transition ($x=0$) or a combined *Q* and rotational transition ($x=1$) takes place in an ortho ($J=1$) or para ($J=0$) molecule. Note that in this frequency range all observed transitions must involve one and only one vibrational quantum.

the Q_P branch at 80 K and an increase in the Q -branch splitting ($\Delta \approx 290 \text{ cm}^{-1}$). The reduced Q_P absorption intensity at low temperature is consistent with Boltzmann statistics expressed in Eq. (2), namely,

$$R \equiv I_{Q_P}(80 \text{ K})/I_{Q_P}(300 \text{ K}) \\ = \exp \left[- \left[\frac{\bar{\Delta} \nu h c}{k} \right] \left[\frac{1}{80} - \frac{1}{300} \right] \right]. \quad (6)$$

Since the Q_P branch is not well defined, an average splitting $\bar{\Delta} \nu \approx 132 \text{ cm}^{-1} \left\{ \frac{1}{2} [\Delta(300 \text{ K})/2 + \Delta(80 \text{ K})/2] \right\}$ is taken, yielding $R=0.17$, which is in good agreement with the measured ratio $R=0.2 \pm 0.1$ at $\nu \approx 4023 \text{ cm}^{-1}$.

The increase in the Q -branch splitting indicates an increase in density, since, according to the kinetic theory,

$$\tau_c \sim N_{\text{H}_2}^{-1} T^{-1/2},$$

the half-width δ_c is proportional [Eq. (1)] to $N_{\text{H}_2} \sqrt{T}$. It was found that both the splitting and intensity of the Q branch at 80 K were consistent with a density $N_{\text{H}_2} \sim 2.7 \times 10^{22} \text{ H}_2/\text{cm}^3$ (≈ 1000 amagat), corresponding to a pressure of 4 kbar (Chabal and Patel, 1984a). The observation that, when thermal contraction occurs, large volume changes ($\Delta V/V \approx 20\%$) can take place, suggests that the H_2 microbubbles are in static equilibrium with the amorphous silicon lattice.

At much lower temperatures ($\sim 10 \text{ K}$), the changes in infrared spectra as a function of time (Fig. 5) have been useful to elucidate the nature of these H_2 pockets (Chabal and Patel, 1984b). Two distinct regions of the spectra evolved with time at different rates. The part of the spectrum that could clearly be identified as a "solid" H_2 spectrum, i.e., characterized only by H_2 single and double transitions, showed an increase of the parahydrogen features with a fast rate $(7 \pm 3) \times 10^{-2} \text{ h}^{-1}$. In contrast, another part of the spectrum that could not be identified as having pure H_2 transitions but rather silicon-modulated H_2 transitions, evolved at a much slower rate $(1.75 \pm 0.1) \times 10^{-2} \text{ h}^{-1}$. These observations indicate that the occluded H_2 can be divided into two general categories, "volume" H_2 and "surface" H_2 , characterized by different environments.

The bimolecular conversion rate constant α , for one-phonon conversion via the nuclear dipole interaction, has the dependence (Graebner *et al.*, 1985)

$$\alpha \sim n_{\text{ph}} \eta / r^8, \quad (7)$$

where n_{ph} is the density of states of phonons with an energy corresponding to 170 K (for bulk H_2 at zero pressure), η is the number of nearest neighbors, and r is the intermolecular separation. The phonon participation in this process is difficult to estimate because of the highly constrained nature of H_2 and the amorphous nature of the surrounding Si. If we assume that the functional form of Eq. (7) holds and that n_{ph} remains the same for all occluded H_2 , then the measured conversion rate differences can be accounted for by a change in the number of nearest

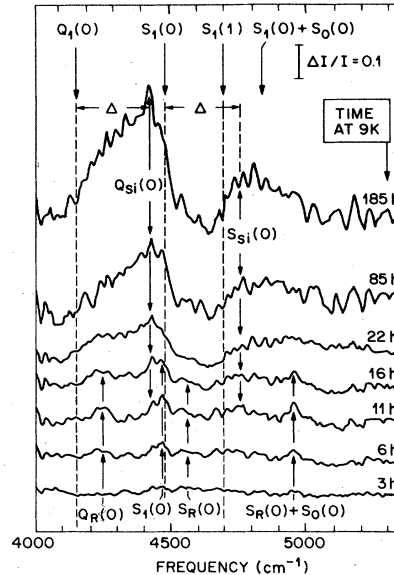


FIG. 5. Time dependence of the H_2 spectrum for a sample held at $T=9 \text{ K}$ obtained by ratioing each spectrum to that taken at time = 0, i.e., $\frac{1}{2}$ h after $T=9 \text{ K}$ was reached (Chabal and Patel, 1984b). In these data, the signal-to-noise ratio degrades with time because of spectrometer instabilities over the period of one week required to take the data. The noise appears as sharp features that extend over the whole spectrum (2000–6000 cm^{-1}). The dashed lines labeled $Q_1(0)$, $S_1(0)$, $S_1(1)$, and $S_1(0) + S_0(0)$ mark the positions of the zero-phonon lines in *unconstrained solid* H_2 . Note the slower increase of phonon sidebands labeled $Q_{\text{Si}}(0)$ and $S_{\text{Si}}(0)$.

neighbors from a maximum of 12 (close-packed solid) to as little as 3.

The measured rates are not accurate enough to separate a bimolecular from an exponential decay. Each of the two rates involves an average over all of the configurations of H_2 within *a*-Si:H, particularly for "surface" H_2 , which will have a variable number of nearest H_2 and Si neighbors. However, the observation of two average rates associated with two distinct spectral regions is a strong confirmation of the presence of clusters of at least 13–15 molecules, i.e., enough to have "volume" H_2 .

With the assumption stated above regarding the phonon density of states, the fast rate observed for the "volume" molecules would suggest that the "solid" H_2 at 9 K is under pressure (smaller intermolecular distance). Several questions therefore arise as to the nature of the expected phase transition from a high-temperature gaseous or liquid phase (fast diffusion, no ordering) to a low-temperature solid phase (limited diffusion and possibly some local ordering).

A strong clue that some phase change associated with the H_2 clusters takes place at low temperatures was provided by comparing IR spectra at different sample temperatures (Fig. 6). Due to the small refractive index mismatch between the *a*-Si:H film ($\epsilon \approx 12$) and the crystalline Si support ($\epsilon \approx 11.7$), small oscillations are present

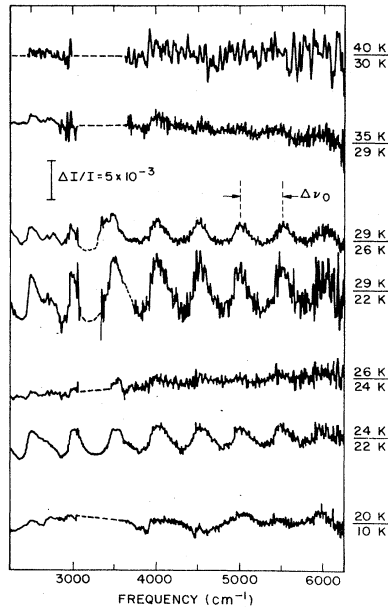


FIG. 6. Representative difference spectra, $I_{T_1}(\nu) - I_{T_2}(\nu)$, for a number of T_1/T_2 ratios taken 120 h after initial cooling (Chabal and Patel, 1984b). The dashed lines represent an uncertain range of data as a result of an increase in water adsorption (on detector and sample) from one run to the next. Note that ratios involving temperatures outside the range 22–29 K display no broadband oscillations. In contrast, ratios involving temperatures in the 22–29 K range display broadband spectral oscillations with period $\Delta\nu_0 \approx 500 \text{ cm}^{-1}$. At very low temperatures, data taken at $T_1/T_2 = 20 \text{ K}/10 \text{ K}$ show some spectral changes at $\nu_0 \approx 4155 \text{ cm}^{-1}$, possibly due to rearrangement of solid H_2 .

in the transmitted spectrum ($\Delta I/I \sim 10^{-2}$). The period, 500 cm^{-1} , arises from the optical path length in the *a*-Si:H film, $2 \times \sqrt{\epsilon} \cos \theta \times (\text{thickness of the } a\text{-Si:H film})$, where $\theta = 33.4^\circ$ is the incidence angle within the *a*-Si:H film. If the thickness of either the crystalline Si substrate or the *a*-Si:H film is changed upon a change ΔT in temperature, then the phase of these spectral oscillations will change and an observable modulation will appear in the intensity ratio $I(T - \Delta T)/I(T)$ over the entire frequency range. Such a modulation was obtained around room temperature and was well accounted for by the expansion of the $500\text{-}\mu\text{m}$ -thick crystalline silicon substrate. However, below 80 K the thermal expansion of *c*-Si is very small and does not provide any modulation for $\Delta T \lesssim 10 \text{ K}$.

The key observation was that, in regions where the substrate expansion is completely negligible, clear oscillations were reproducibly detected over the whole frequency region for $\Delta T \sim 3 \text{ K}$ over a very specific temperature range, $T = 22\text{--}29 \text{ K}$. Above and below this range, no such oscillations were present. The most straightforward explanation is a change in thickness ($\approx 0.02\%$) of the *a*-Si:H film. This change presumably arises from a change in volume of the H_2 bubbles which, from the estimated H_2 concentration, would be of the order

$\Delta V/V \approx 2\%$. The IR measurement cannot distinguish between a contraction or an expansion of the bubbles upon cooling, but it is reasonable that a contraction occurs upon "solidification." The nature of this transition will be discussed further in Sec. V after the more recent NMR data are reviewed.

It would appear therefore that the volume of the microcages containing H_2 can vary. The fact that the surrounding *a*-Si matrix is not rigid but rather can accommodate variations in the H_2 state is consistent with several observations pointing to the compressed nature of the solid H_2 . These observations include the high ortho-para conversion rate for the "volume" H_2 , specific shifts of spectral features from the zero-pressure position, and width of bands at low temperatures. None of these observations is a proof by itself, since little is known about the ortho-para conversion and optical absorption of *highly constrained* solid H_2 , but the existence of a high density of the solid H_2 provides the most natural explanation of all these phenomena. Such high pressures at low temperatures would be inconsistent if the microcages retained the same geometry (except for a small thermal contraction) with the 2-kbar pressure measurement at room temperature.

IV. RECENT NMR STUDIES: NATURE OF H_2 IN THE TRANSITION REGION

A new effort using NMR to study H_2 in *a*-Si:H was started by Lamotte (1984), who used magic angle spinning (MAS) in an attempt to resolve the narrow component of the NMR signal. A typical *a*-Si:H sample exhibits a narrow and a broad component in the frequency domain [i.e., the Fourier transform of the free-induction-decay (FID) signal] as shown by Reimer *et al.* (1981). The broad component has been attributed to protons (SiH , SiH_2 , ...) clustered in aggregates, resulting from chemical shift dispersion and strong proton-proton interactions. The narrow line, on the other hand, is believed to be due in part to isolated SiH , which has small proton-proton interactions, and also to molecular H_2 . By using MAS, Lamotte averaged out all orientational anisotropies in the narrow component while leaving the broad component unaffected. He argued that a very narrow resonance (linewidth $\approx 160 \text{ Hz}$) occurring at 4.5 ppm (within the narrow line) could be identified with molecular H_2 in *a*-Si:H.

This assignment is somewhat controversial. If most of the narrow component were due to molecular H_2 , then one would expect to observe motional narrowing of this component with increasing temperature. This has not been borne out by other experiments (Carlos *et al.*, 1985). In unannealed samples, Boyce and Stutzmann (1985) have presented evidence that gaseous H_2 contributes to a negligible fraction of the narrow line. Recently, Zumbulyadis (1986) used a two-dimensional Fourier-transformed NMR technique to study the origin of the narrow line at room temperature. By monitoring the cross polarization and

magic-angle-spinning spectrum of ^{29}Si , he demonstrated that for at least one typical *a*-Si:H sample (hot wall, rf plasma-enhanced chemical vapor deposition) the narrow component originates from hydrogen bonded to silicon in the lattice and dipolarly coupled to adjacent silicons. Some of the discrepancy may therefore arise from the study of samples prepared in different ways. The influence of sample preparation is important in comparing the results of different experiments and will be discussed in the next section.

More recently, Boyce and Stutzmann (1985) were able to observe H_2 with NMR directly by detecting a powder-averaged Pake doublet (175-kHz splitting) of an *orientationally ordered* phase of H_2 at low temperatures (Fig. 7). This doublet arises from the presence of orthohydrogen placed in a crystal field. As a result of this field, the degeneracy of the three m_J levels ($J=1, m_J=0, \pm 1$) of orthohydrogen is lifted. In normal solid H_2 below 1.6 K, a splitting of 165 kHz is observed, which is the result of mostly EQQ interactions. In *a*-Si:H, there is a distribution of local environments and the relevant crystal-field splitting is the mean value, probably dominated by electric field gradients (EFG). Assuming an axially symmetric EFG and averaging over the distribution of angles with respect to the applied magnetic field (powder average), singularities are expected at ± 86.5 kHz about the $m_J=0$ level, in good agreement with the observed splitting. The H_2 phase is therefore *orientationally ordered with respect* to local fields, predominantly EFG arising from the *a*-Si matrix, and not necessarily with respect to other H_2 molecules.

The ordering transition temperature T_c , defined as the loss of the Pake doublet, is found to be lower for the postannealed samples ($T_c \approx 10$ K) than for the unannealed samples ($T_c \approx 20$ K). The argument to explain the

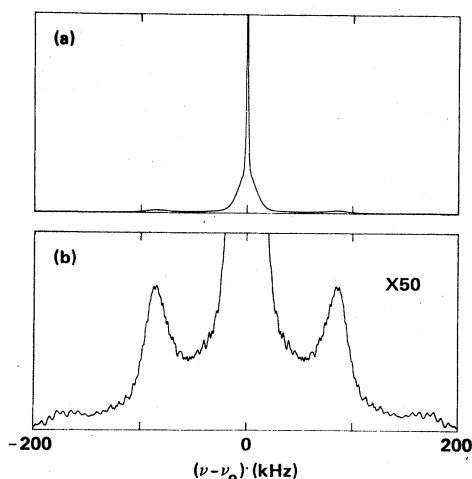


FIG. 7. Proton NMR spectrum for a Fourier transform of the free-induction decay at 92 MHz and $T=1.43$ K in a sample annealed at 500°C measured by Boyce and Stutzmann (1985). The spectrum shows (a) the broad and narrow central lines (top) and (b) the molecular H_2 powder pattern with broadened singularities at $\pm(88 \pm 5)$ kHz (bottom).

various critical temperatures is based on the effect of the *a*-Si matrix EFG on T_c . The larger the EFG, the higher T_c , because the averaged value of the splitting is increased. This conclusion is supported by the fact that the annealed samples have more H_2 (≈ 1 at. %) than the unannealed samples (≈ 0.25 at. %), as measured from the spectral area under the Pake doublet, and therefore are less affected by the *a*-Si EFG.

Very recently, however, Fedders (1987a, 1987b) has argued that orientational ordering of H_2 in microvoids is unlikely above the critical temperature of bulk single-crystal H_2 . The origin of the Pake doublet is attributed instead to a slowing down of the phonon-induced relaxation rate among the molecular m_J states of orthohydrogen. When this rate is less than the nuclear spin-molecular coupling frequency, the Pake doublet appears. Since the rate varies as T^7 at low temperatures (Leopold *et al.*, 1985), a very sharp onset of the Pake doublet will occur, as observed experimentally by Boyce and Stutzmann (1985). This interpretation stresses the relative importance of strong EFG in *a*-Si with random orientation. An orientationally ordered state with an associated critical temperature is not compatible with such a picture.

Above the temperature at which the Pake doublets disappear, a melting transition is expected. The melting is measured by NMR as an increase in diffusion. When the hopping rate of the H_2 molecules is comparable to their NMR linewidth, then the intermolecular interaction is averaged out and a motional narrowing is observed. Boyce and Stutzmann (1985) observed such a narrowing for the annealed samples between 15 and 40 K, i.e., above the melting temperature of pure solid *n*- H_2 , $T_m=14$ K. This range (15–40 K) is consistent with a solid under a range of pressures, 0–2 kbar, and is remarkably similar to the phase transition observed in the IR measurements (22–29 K) by Chabal and Patel (1984b).

The picture that emerges from this NMR work is that the occluded H_2 solidifies (reduced diffusion) around 27 K. At lower temperatures (≤ 10 K for the postannealed samples), a Pake doublet appears that can be interpreted as orientational ordering or as simply a decrease of the phonon-induced relaxation rate. No T_m measurements could be done on the unannealed samples due to the small fraction of H_2 contributing to the narrow line.

Another aspect of the NMR measurements concerning the concentration of H_2 in *a*-Si:H is also clarified (Boyce and Stutzmann, 1985; Fedders *et al.*, 1985). From proton NMR relaxation time measurements, consistently smaller amounts of H_2 were deduced compared to what was found by other measurements. A large fraction of the occluded H_2 is now known to be in high-density form with a $T_1(\text{H})$ dominated by EQQ interactions (i.e., with no T_1 minimum). Fedders *et al.* (1985) have shown that the previously observed T_1 did not reflect these H_2 dominated by EQQ interactions (i.e., "volume" H_2), but rather arose from a smaller fraction of the H_2 with a small EQQ interaction and large static EFG of low symmetry. This subset of H_2 , which is effectively dilute as far as nuclear relaxation is concerned (negligible EQQ interactions), is

naturally explained as the "surface" H_2 in contact with the *a*-Si:H matrix, i.e., at the surface of the H_2 bubbles.

Additional information on the nature of the *a*-Si matrix in the vicinity of the voids was obtained from a deuteron and proton NMR study performed on a number of differently prepared samples (Leopold *et al.*, 1985). Because the deuterium nucleus has a spin of 1 and a low gyromagnetic ratio, the interaction of the quadrupole moment with EFG in a solid will give rise to a NMR spectrum characterized by a powder-averaged Pake doublet with little dipole broadening. As a result, the line shape can be decomposed clearly into different components associated with deuterium in different *local* environments. Leopold *et al.* (1985) extracted three different components in the deuteron magnetic resonance (DMR) line shapes: a resolved powder-averaged Pake doublet associated with D bonded to Si well removed from microvoids, a wide quadrupole-broadened central line associated with D located near and on the surfaces of microvoids, and a sharp temperature-dependent feature associated with molecular D_2 in the larger voids.

The splitting of the Pake doublet associated with D bonded to Si (66 KHz) can be related to the observed vibrational stretching mode of SiD ($\approx 1460 \text{ cm}^{-1}$). The broad central component corresponds to a more clustered deuteron configuration than the isolated SiD, possibly because of the greater strain and disorder around the rough microvoid. These more-clustered deuterium nuclei are characterized by a faster dipolar damping than the isolated SiD because they are located closer to the molecular D_2 . The sharp central component is motionally narrowed in a temperature range comparable to that observed by Boyce and Stutzmann (1985). Both the strength and the melting temperature varied from sample to sample, confirming that the sample preparation can affect the total amount of trapped D_2 .

In yet unpublished work, Fry *et al.* (1987) have carried out spin-echo measurements combined with T_1 measurements on a variety of samples. The merit of spin-echo T_2 measurements is to isolate protons on the basis of their homonuclear dipolar interactions: fast T_2 decay for protons with strong coupling and slower T_2 decay for protons with weaker coupling.

Fry *et al.* find that the protons with slow T_1 decays are characterized by fast T_2 decays and correspond to "isolated" monohydride species. In contrast, the protons with fast T_1 decays and slow T_2 decays may be associated with molecular H_2 . If so, then the measured decay of the magnetization echo ($T_2 > 10 \text{ msec}$) for the H_2 molecules gives an upper limit on homonuclear dipolar and quadrupolar interactions or lifetime broadening experienced by the H_2 molecules. For gaseous H_2 , the quadrupolar interactions are negligible, and they estimate that H_2 must be at least 10 Å from nearest-neighbor atomic H (e.g., SiH). Thus they infer that molecular H_2 reside in SiH-covered voids having a diameter of at least 20 Å, or in single proton-free voids with nearest-neighbor protons $> 10 \text{ Å}$ away.

More importantly, Fry *et al.* (1987) found that the

amount of occluded H_2 is not correlated either to the electronic quality of the sample or to the total H concentration, but rather depends on the deposition and annealing parameters. In the next section we will discuss various aspects of this occluded H_2 using mostly results obtained on "good" glow discharge samples. However, even with this method of preparation ($T_s \approx 230^\circ\text{C}$, 5 W), differences in final H_2 concentration are found, due mostly to gas composition and deposition rate, and should be kept in mind.

V. DISCUSSION

A. Nature of microvoids in *a*-Si:H

A direct implication of the discovery of dense H_2 in *a*-Si:H is the presence of microvoids. The nature of these microvoids can be inferred indirectly from all the studies of H_2 in *a*-Si:H. For instance, an estimate of the size can be obtained assuming a spherical geometry. From bimolecular decay measurements, calorimetry experiments set a lower limit at 10 H_2 (to 20 H_2) giving a 10-Å diam (Graebner *et al.*, 1985). The IR measurements showed that "bulk" H_2 was present, which required 12 H_2 –15 H_2 ($d \approx 10 \text{ Å}$) as a minimum. The surface-to-volume- H_2 ratio obtained from low-temperature IR spectra implied that no more than 100 H_2 on average were trapped in a single void (Chabal and Patel, 1984b). That would set an average upper limit at $d \approx 20 \text{ Å}$. The same reasoning was applied to the recent NMR data, with the surface molecules having been obtained from the T_1 measurements. A surface-to-volume ratio of 0.4 to 0.2 was estimated, giving a diameter of order 20–40 Å. Calorimetry and NMR experiments were performed on samples similarly grown (100% SiH_4 , 2 W), while the IR measurements were performed on samples of plasma deposited in slightly different conditions (30% SiH_4 , 70% Ar, 0.36 Torr at 5 W). Both sets yielded an excellent electronic quality (Graebner *et al.*, 1985).

Estimates of the void size range therefore from 10 to 40 Å diam. This number is slightly larger than what would have been expected from small-angle neutron scattering (SANS) experiments performed on similarly grown films (Leadbetter *et al.*, 1981). In SANS, the mean-square fluctuation of the scattering length is measured by an appropriate integral of the measured scattering intensity over reciprocal space. For samples relevant to this study, no inhomogeneities could be measured within the resolution, i.e., the root mean square of the structures is of order 10 Å or less. Combining all the above results, one may take the range 10–20 Å as the most probable size (diameter for spherical shape) of the microstructures. No measurements, however, unambiguously exclude the possibility of wide fluctuations about this average value, as suggested by Bork *et al.* (1986). For instance, surface molecules could be due mostly to very small or long voids ($\approx 5 \text{ Å}$ diam, if spherical; 5–40 Å long, if cylindrical),

while volume molecules could originate from large voids (≈ 50 Å). Long cylinders or large voids would then be in low enough concentrations not to be detectable by SANS.

SANS measurements on samples prepared by cathode plasma deposition on room-temperature substrates uncovered a marked increase in inhomogeneity with no loss of H upon annealing to 375°C, suggesting that hydrogen can migrate within a noncolumnar structure and be trapped as H₂ in internal pores instead of being released (Leadbetter *et al.*, 1981). There is therefore evidence that the microvoid distribution and morphology change upon relatively small temperature variations. While it is clear that annealing above room temperature produces such modifications, partly due to H diffusion, it also appears that changes occur upon cooling below room temperature. The evidence is indirect (see Sec. III.B) and relies mostly on the fact that, if H₂ is under 2-kbar pressure at room temperature and also under pressure at low temperature (solid form), then an overall decrease of the voids volume must take place, as inferred from the data presented in Fig. 4.

The stress measurements of Harbison *et al.* (1984) may help account for such anisotropic morphology variations. Using a bending-beam method, the *a*-Si:H bulk modulus is measured by detecting the bowing present on a thin *c*-Si substrate after a 0.5–2- μ m-thick film is grown on one side only. The results show that *a*-Si films grow under high compressive stress, as high as 800 MPa (≈ 8 kbar) for low silane concentration in the plasma. For the films used in the IR experiments, typical compressive stresses corresponding to 1–2 kbar are reported.

Such a value for the average compressive stress suggests that the occluded H₂ pockets will respond to a change, e.g., upon thermal contraction, by a change in pressure. Alternatively, the *a*-Si film can expand or contract upon a H₂ pressure change. Support for the latter comes from the observed phase transition by the IR interference method (Chabal and Patel, 1984b). Thus, while H diffusion may account for most of the morphology changes above room temperature, an anisotropic type of relaxation may account for changes inferred below room temperature. Accurate H₂ density measurements may be a sensitive measure of *a*-Si:H film mechanical stability in the range relevant for solar-cell operation (300–600 K).

The observation of H₂ bubbles in bulk material is not unique to *a*-Si. Schwark *et al.* (1983) showed that H₂ bubbles were occluded in Cu by measuring the heat released during ortho-para conversion at low temperature. The amount of H₂ necessary to explain their data was 10–100 ppm, and appeared to be trapped in large voids (≈ 4000 Å) under low density ($\approx 10^{10}$ H₂/cm³). High-density bubbles have been observed in Al upon Ne, Ar, and Xe implantation (Vom Felde *et al.*, 1984). The density of the bubbles was determined from the pressure shift of the ¹S₀-¹P₁ transition of the rare gases and from electron diffraction patterns. The results show overpressurized bubbles (≈ 100 kbar) containing liquid Ne, Ar, and Xe at room temperature. The formation of these high-density bubbles also requires diffusion and nucleation.

B. Hydrogen phase transitions and low-temperature phases

As the *a*-Si:H samples are cooled down, a phase transformation takes place, as seen by IR interference experiments in the range 22–29 K (Chabal and Patel, 1984b) and by a broadening in the NMR lines in the range 15–40 K (Boyce and Stutzmann, 1985). The IR observation was reported for measurements taken 120 h after initial cooling and was found to be independent of the ortho-para concentration. It is therefore unlikely to be an intrinsic H₂ orientational phase transition but rather a “freezing” of the H₂ molecules as confirmed by the NMR data.

The range of temperatures over which this transition occurs is the strongest evidence for a high-pressure liquid-to-solid transition. Recently, Adams *et al.* (1984) have shown that the melting temperature T_m of ⁴He in confined geometries was lowered compared to that of unconstrained ⁴He. Therefore one would expect the melting temperature of H₂ to be lowered, due to the highly confined environment, below that of H₂ under similar pressures in unconfined geometries. The observation of a phase transition above 25 K, i.e., well above the zero-pressure temperature $T_m = 14$ K (McCarty, 1975), strongly suggests that it involves a transition to a solid under high pressure. The characteristic sharpening of the IR spectra expected for a liquid-to-solid transition at zero pressure (Gush, 1960) is absent (Chabal and Patel, 1984b), which also suggests a liquid-to-solid transition at high pressures.

The transition to an orientational ordered state taking place at lower temperatures (10–20 K) only involves the orthohydrogen and is therefore expected to be strongly dependent on the ortho-para concentration (Boyce and Stutzmann, 1985). More insight into this low-temperature phase would be obtained if the NMR measurements of Boyce and Stutzmann could be repeated as a function of ortho-para concentration. Calorimetry experiments have shown that there is an excess entropy in this low-temperature phase attributed to a lack of long-range order (Graebner *et al.*, 1985). The ground state of the unconstrained solid *n*-H₂ is an array of ortho molecules with long-range orientational order on an fcc lattice (Silvera, 1980). In *a*-Si:H, the solid H₂ appears to have no long-range order (Graebner *et al.*, 1985), and yet there is a well-defined local orientational arrangement to give rise to a dipolar powder pattern in the NMR experiment. If, as suggested by Graebner *et al.* (1985), the H₂ solid is frozen in a quadrupolar glass structure below 2 K, then the powder-averaged Pake doublet cannot arise from intrinsic H₂ orientational order but rather from a local ordering with respect to EFG of the *a*-Si.

In conclusion, the nature of the solid H₂ phase in *a*-Si at low temperature, particularly below 10 K, is far from being understood. Hydrogenated *a*-Si may be the only system in which a compressed phase of H₂ in a highly restricted geometry can be studied. As the formation of the microvoids is better understood, this strange state of

matter may be studied more reliably. It is likely that NMR will continue to play an important role in this research. However, other experiments could be of great value. Cross-section scanning electron microscopy may be able to image the microvoids (Knights, 1985; Musket *et al.*, 1986; Tsai *et al.*, 1986). High-energy electron diffraction could be performed in an attempt to establish the degree of ordering of this solid. Stress measurements at low temperature may be able to confirm the liquid-to-solid phase transitions. Infrared photoacoustic and Raman scattering experiments would complement the existing IR measurements. The story of H₂ in *a*-Si is far from complete.

ACKNOWLEDGMENTS

The authors are grateful to T. M. Duncan, J. E. Graebner, and L. W. Jelinski for a critical reading of this paper.

REFERENCES

- Adams, E. D., K. Uhlig, Yi-Hua Tang, and G. E. Haas, 1984, *Phys. Rev. Lett.* **52**, 2249.
- Bork, V. P., P. A. Fedders, D. J. Leopold, R. E. Norberg, J. B. Boyce, and J. C. Knights, 1986, *Mater. Res. Soc. Proc.* **70**, 89.
- Boyce, J. B., and M. Stutzmann, 1985, *Phys. Rev. Lett.* **54**, 562.
- Boyce, J. B., and M. J. Thompson, 1984, *J. Non-Cryst. Solids* **66**, 127.
- Cardona, M., 1983, *Phys. Status Solidi B* **118**, 463.
- Carlos, W. E., J. A. Reimer, and P. C. Taylor, 1985, *Phys. Rev. Lett.* **54**, 1205 (comment) and reply by B. Lamotte, *ibid.*, p. 1206.
- Carlos, W. E., and P. C. Taylor, 1980, *Phys. Rev. Lett.* **45**, 358.
- Carlos, W. E., and P. C. Taylor, 1982, *Phys. Rev. B* **25**, 1435.
- Chabal, Y. J., and C. K. N. Patel, 1984a, *Phys. Rev. Lett.* **53**, 210.
- Chabal, Y. J., and C. K. N. Patel, 1984b, *Phys. Rev. Lett.* **53**, 1771.
- Chabal, Y. J., and C. K. N. Patel, 1985, *J. Non-Cryst. Solids* **77&78**, 201.
- Conradi, M. S., K. Luszczynski, and R. E. Norberg, 1979, *Phys. Rev. B* **20**, 2594.
- Conradi, M. S., and R. E. Norberg, 1981, *Phys. Rev. B* **24**, 2285.
- Dexter, D. L., 1955, *Phys. Rev.* **101**, 48.
- Fedders, P. A., 1979, *Phys. Rev. B* **20**, 2588.
- Fedders, P. A., 1987a, *Bull. Am. Phys. Soc.* **32**(3), 587.
- Fedders, P. A., 1987b, *Phys. Rev. B* **36**, 2107.
- Fedders, P. A., R. Fisch, and R. E. Norberg, 1985, *Phys. Rev.* **31**, 6887.
- Fry, C. G., T. M. Apple, and B. C. Gerstein, 1987, "Quantitative determination of molecular hydrogen in *a*-Si:H using proton NMR," Ames Laboratory-USDOE and Dept. of Chemistry-Iowa State University Preprint.
- Graebner, J. E., L. C. Allen, and B. Golding, 1985, *Phys. Rev. B* **31**, 904.
- Graebner, J. E., B. Golding, L. C. Allen, D. K. Biegelsen, and M. Stutzmann, 1984, *Phys. Rev. Lett.* **52**, 553.
- Gush, H. P., W. F. Hare, E. J. Allin, and H. L. Welsh, 1960, *Can. J. Phys.* **38**, 176.
- Harbison, J. P., A. J. Williams, and D. V. Lang, 1984, *J. Appl. Phys.* **55**, 946.
- Hare, W. F. J., and H. L. Welsh, 1958, *Can. J. Phys.* **36**, 88.
- Knights, J. C., 1985, *Mater. Res. Soc. Symp. Proc.* **38**, 371.
- Kriegler, R. J., and H. L. Welsh, 1968, *Can. J. Phys.* **46**, 1181.
- Lamotte, B., 1984, *Phys. Rev. Lett.* **53**, 576.
- Lamotte, B., 1985, *J. Non-Cryst. Solids* **77&78**, 191.
- Lax, M., 1952, *J. Chem. Phys.* **20**, 1752.
- Leadbetter, A. J., A. A. M. Rashid, N. Colenutt, A. F. Wright, and J. C. Knights, 1981, *Solid State Commun.* **38**, 957.
- Leopold, D. J., J. B. Boyce, P. A. Fedders, and R. E. Norberg, 1982, *Phys. Rev. B* **26**, 6053.
- Leopold, D. J., B. S. Coughlan, P. A. Fedders, R. E. Norberg, J. B. Boyce, and J. C. Knights, 1984, *J. Non-Cryst. Solids* **66**, 121.
- Leopold, D. J., P. A. Fedders, R. E. Norberg, J. B. Boyce, and J. C. Knights, 1985, *Phys. Rev. B* **31**, 5642.
- Löhneysen, H. V., J. H. Schink, and W. Beyer, 1984, *Phys. Rev. Lett.* **52**, 549.
- McCarty, R. D., 1975, in *Hydrogen; Its Technology and Implications: Hydrogen Properties*, edited by K. E. Cox and K. D. Williamson (The Chemical Rubber Company Press, Boca Raton), Vol. 3, p. 59.
- Musket, R. G., D. W. Brown, and R. F. Pinizzotto, 1986, *Appl. Phys. Lett.* **49**, 379.
- Norberg, R. E., 1985, *Phys. Rev.* **31**, 7925.
- Onsager, L. J., 1936, *Am. Chem. Soc.* **58**, 1486.
- Reimer, J. A., R. W. Vaughan, and J. C. Knights, 1981, *Phys. Rev. B* **24**, 3360.
- Schwark, M., F. Pobell, W. P. Halperin, Ch. Buchal, J. Hanssen, M. Kubota, and R. M. Mueller, 1983, *J. Low Temp. Phys.* **53**, 685.
- Silvera, I. F., 1980, *Rev. Mod. Phys.* **52**, 393.
- Taylor, P. C., 1984, in *Semiconductors and Semimetals*, edited by J. I. Pankove (Academic, Florida), Vol. 21, Part C, p. 99.
- Tsai, C. C., J. C. Knights, G. Chang, and B. Wachter, 1986, *J. Appl. Phys.* **59**, 2998.
- Vander Heiden, E. D., W. D. Ohlsen, and P. C. Taylor, 1984, *J. Non-Cryst. Solids* **66**, 115.
- Van Kranendonk, J., 1968, *Can. J. Phys.* **46**, 1173.
- Vom Felde, A., J. Fink, Th. Müller-Heinzerling, J. Pflüger, B. Scheerer, G. Linker, and D. Kaletta, 1984, *Phys. Rev. Lett.* **53**, 922.
- Zumbulyadis, N., 1986, *Phys. Rev. B* **33**, 6495.